

# Tunable Amplitude and Phase Modulation in Terahertz Regime Using Transverse Stratified Configuration

Daniele Lo Forti<sup>1</sup>, Robert G. Lindquist<sup>1, \*</sup>, and Martin S. Heimbeck<sup>2</sup>

**Abstract**—A number of transverse stratified configurations of metal and dielectric layers are studied for modulating Terahertz radiation in amplitude and phase. Pass band flat-top response and high wide-band transmission is achieved by means of a metallic grating filled with Liquid Crystal (LC) in different configurations and with the use of either grazing angles of incidence or cuts pierced within the grating. The transverse configuration with thin LC films allows for high speed tunability with low applied voltage. A dielectric grating with non-continuous electrodes is studied showing wide pass band response suitable for phase modulation applications.

## 1. INTRODUCTION

In the past two decades, research into the terahertz (THz) regime for applications in the medical and defense sectors has been growing rapidly. The ability to accurately tune the amplitude and/or phase of a THz wave would be of great benefit to improve imaging, communications, beam steering, sensing, and filtering devices. The current technology to manage electromagnetic radiation in the terahertz regime uses mesh-based devices, but this technique is not tunable. A number of configurations utilize mechanically tunable devices, e.g., the use of two parallel plate waveguides (PPWGs) tuned with two sliding metal plates [1] or a homeotropically aligned liquid crystal (LC) cell tuned with a rotating magnet [2]. Mechanically tuned devices have significant limitations in size, more complex manufacturing process and significantly lower speeds than electrically tuned ones. Some improvement has been achieved with MEMs devices, for example a 65% modulation over 1.5 THz has been achieved with the use of a two layer reconfigurable mesh filter [3]. Tunability of the normally incident field is obtained by reducing the spacing between two orthogonally aligned linear structures. In [4] by Zhu et al., a notching effect is realized by decreasing the spacing between a series of half square pairs by means of a comb drive. The attenuation at the notch can reach 25 dB with a tunability of 0.48 THz.

Electro-optic techniques to tune the amplitude and/or phase of an electromagnetic wave are commonplace in the visible and the infrared regimes; however, these techniques have had limited use in the longer wavelength regimes such as the THz region. The idea of using an electrically controlled birefringence (ECB) LC cell to phase modulate an incoming signal has been studied by Wu et al. [5], where tunability of a 1.83-mm-thick vertically aligned nematic liquid crystal (NLC) cell is demonstrated. Although the cell was able to phase shift an incoming signal up to a full wave, the voltage required was 100 V and the response of this LC device was as slow as a mechanical solution due to the thickness of the LC layer. To improve the speed, the thickness of the LC layer must be significantly reduced. This can be achieved by using zero-order gratings similar to the work by Yang and Sambles [6] in the microwave regime. A zero-order grating of metallic slabs with a 75  $\mu\text{m}$  homogeneously aligned layer of

---

*Received 20 September 2014, Accepted 10 November 2014, Scheduled 27 December 2014*

\* Corresponding author: Robert G. Lindquist (lindqr@uah.edu).

<sup>1</sup> Engineering and Computer Engineering Department, University of Alabama in Huntsville, Huntsville, AL, USA.

<sup>2</sup> Charles M. Bowden Research Center, Army Aviation & Missile RD&E Center, Redstone Arsenal, AL 35898, USA.

LC in between to exploit tunable wavelength selection properties at microwave frequencies allowed for a high tunability at low voltages but it reduced the transmittivity to 20% or less.

In this paper, an effective solution is presented to modulate THz radiation by means of a transverse stratified structure that can achieve extensive tunability both in amplitude and phase with low loss. The two configurations studied are a metallic grating and a dielectric grating. The former consists in a grating of metal plates interleaved with thin layers of liquid crystal. The presence of the metal makes the device highly reflective for most frequencies; the only frequencies that are not reflected follow the Fabry-Perot etalon theory. This natural characteristic of the device can be obviously tuned using the LC films. By using techniques like cascade configurations, incidence at grazing angles or excitation coupled Bragg modes within the LC film, the device can be configured for high transmission flat-top narrow pass-band filters, steep amplitude modulators or broadband pure phase modulators. The second configuration is obtained by substituting the metal electrodes with a dielectric coated with two thin metal electrodes. The narrowband resonant transmission characteristic of the first configuration is replaced with a resonant narrowband reflection profile. The transmission has a train of notch filters which can be flattened by cutting the metal layer orthogonally to the direction of propagation making the device better suited for broadband phase modulation.

## 2. METALLIC GRATING

The first configuration studied is a set of metal plates separated by a thin layer of a tunable dielectric as shown in Figure 1. The period of the metallic grating is shorter than half a wavelength at the frequencies of interest in order to allow only for the transmission of the zeroth-order diffraction. The thickness of the dielectric is also sub-wavelength and the lateral size of the grating is large such that each pair of metal plates behaves as a parallel plate waveguide. The only non-evanescent mode within the waveguide is the  $TM_0$ . The dielectric in between the plates is a LC material. In the configuration, each liquid crystal layer and the two metal plates adjacent to it form a homogeneously aligned ECB cell with the director axis initially aligned in the direction of THz wave propagation. When a small ac voltage is applied to the electrodes, the induced field rotates the director axis of the LC away from the wave propagation direction by an angle of  $\theta$  as shown in Figure 1. Due to the highly anisotropic nature of the LC, this change results in a consistent variation of the LC permittivity with the voltage applied as detailed in the next section.

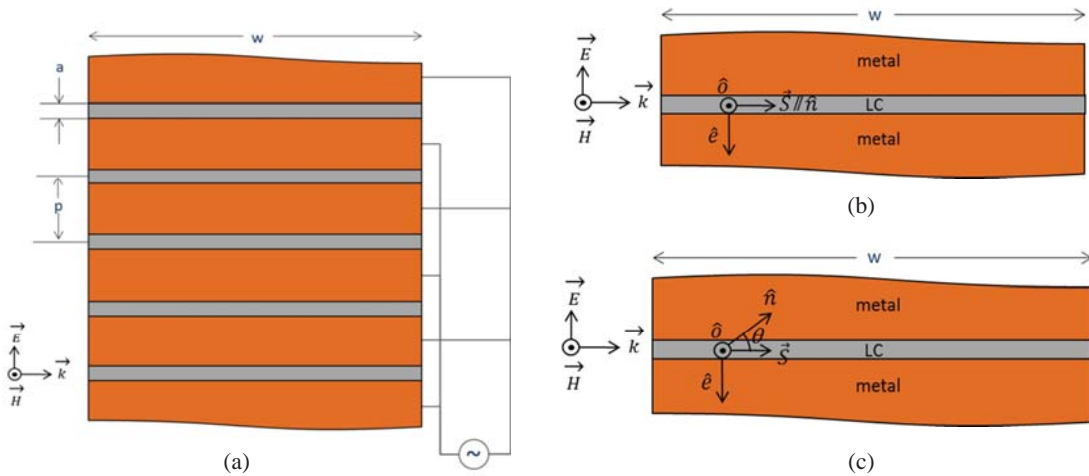


**Figure 1.** (a) Metallic grating geometry and propagation. (b) Orientation of the LC director axis with no voltage applied. (c) Orientation of the LC director axis with voltage applied.

Due to the subwavelength nature of this grating, this configuration could be considered as a pseudo metamaterial with effective refractive index equal to the combination of the metal and LC refractive indices.

## 2.1. Normal Incidence

When radiated with a TM wave at normal incidence, as shown in Figure 1, the wave encounters a high impedance mismatch at the air-grating interface. The high refractive index of metal at THz frequencies causes the equivalent refractive index to increase significantly with respect to the LC index. For instance, the magnitude of the refractive index of good conductors as Copper or Aluminum can reach  $\sim 2000$  or more at THz frequencies. The high mismatch causes a large reflection at both the entrance and exit of the grating forming an etalon; therefore, the only frequencies that are transmitted at the output interface correspond to the etalon's resonance frequencies. Standard Fabry-Perot (FP) theory provides the following formula to calculate resonance frequencies for an etalon:  $2nw = m\lambda$  where  $n$  is the refractive index of the grating,  $w$  is the length of the grating, and  $m$  is a positive integer. The resonance frequencies in this particular configuration are slightly shifted with respect to the FP formula due to the presence of a grating instead of the usual etalon's mirrors. As noted by Medina et al. [7], the two interfaces have the effect of increasing the electrical length of the etalon causing the resonance frequencies to red shift slightly. For this reason, as a first approximation, the device can be modeled as an etalon with reflection coefficients calculated using the index mismatch at the interfaces and length equal to the equivalent electrical length of the channel.

The field in the grating is confined within the dielectric and excites only evanescent modes within the metal due to its very small skin depth at THz frequencies. As previously stated, the only propagating mode in between the plates is the  $TM_0$  with propagation vector parallel to the plate surface. Propagation in each slit can be calculated separately given that each initial phase factor when recombined at the output interface is considered. In other words, the device acts as a space fed linear array antenna in which each LC cell is a radiating element.

When applying a field between the electrodes, the properties of the liquid crystal dielectric in between the plates change. The liquid crystal is an anisotropic uniaxial medium and its permittivity is a tensor. Calculations of the propagation within the medium are simplified by using the ordinary and extraordinary ray method as shown in [8]. Due to this particular geometry in which the director axis is parallel to the propagation vector, the medium behaves isotropically with constant refractive index  $n$  perpendicular ( $n_{\perp}$ ). When the LC medium is excited by an applied voltage, the director axis,  $\hat{n}$ , rotates as shown in Figure 1. The LC medium takes the form of an uniaxial crystal with linear eigenpolarization states known as the ordinary and extraordinary ray. The ordinary ray,  $\hat{o}$ , is perpendicular to the plane of the pointing vector  $\hat{S}$  and  $\hat{n}$  while the extraordinary ray  $\hat{e}$  is perpendicular to the plane of  $\hat{S}$  and  $\hat{o}$ . With some approximations, propagation can be calculated by decomposing the incoming electric field  $E$  into its components along the  $\hat{e}$  and  $\hat{o}$  rays. Due to the use of TM excitation at normal incidence, the  $E$  field couples completely into the  $\hat{e}$  ray with refractive index function of the angle  $\theta$ . The effective refractive index for the extraordinary ray can be calculated using Equation (1):

$$n_e = \sqrt{n_{\perp}^2 \cos^2 \theta + n_{\parallel}^2 \sin^2 \theta} = \sqrt{\epsilon_R} \quad (1)$$

The actual distribution of the LC director axis is determined by the electrostatic torque forces and the elastic torque forces. The relation between the applied field and the director axis distribution is described by a nonlinear differential equation solved in [8].

The propagation can be calculated as if the medium was isotropic with tunable refractive index because all the power couples into the extraordinary ray for this configuration.

Measurements of the capacitance variation with applied voltage for a single ECB cell have been performed. The capacitance has a steep variation when the applied voltage is between 1 V and 2.5 V and continues to increase asymptotically afterwards as shown in Figure 2(a). The typical E7 birefringence is equal to about 11.0 at 1 kHz. The difference between the maximum and minimum capacitance can be formulated as  $\Delta C = \epsilon_0 * \Delta\epsilon * A/d$ , where  $\Delta\epsilon$  is the birefringence,  $A$  the area, and  $d$  the cell thickness. By inverting this formula and using the measured values for  $C$  and the manufacturer value for  $d$  the resulting area is  $\sim 0.9 \text{ cm}^2$ , which is in agreement with the approximately  $1 \text{ cm} \times 1 \text{ cm}$  area that has been filled with LC. Using this more accurate value for the area, LC permittivity is calculated and plotted in Figure 2(b) as a function of applied voltage. Note that this permittivity is measured at 1 kHz. For this reason, the expected values at 1 THz have been added on the right side of the plot as reference.

A suitable LC for THz applications is E7. Measured values of the E7 refractive index at frequencies between 0.2 and 2 THz are 1.690 to 1.704 for  $n_{\parallel}$  and 1.557 to 1.581 for  $n_{\perp}$  at 26°C [9]. The absorption

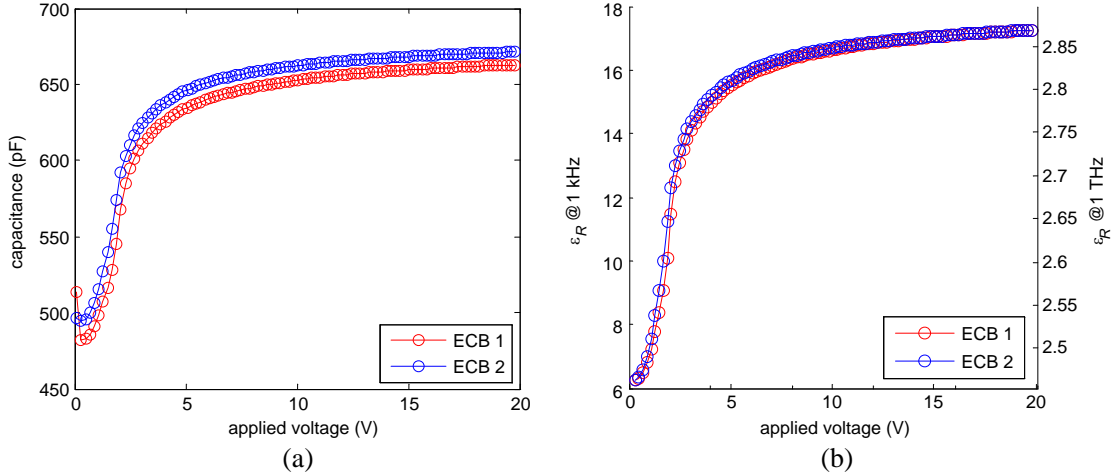


**Figure 2.** (a) Capacitance variation versus 1 kHz applied voltage for Brass + E7 ECB cells. (b) Estimated permittivity variation with voltage at 1 kHz and 1 THz.

coefficient is lower than  $5 \text{ cm}^{-1}$  at the frequencies of interest, and it is considered negligible. For this reason, in the following the LC is considered as a non-lossy material with permittivity equal to the square of its refractive index. When the calculation does not involve tunability of the LC, an average value of  $n = 1.6726$  or  $\epsilon_R = 2.6490$  will be used. The metal used for the electrodes is copper with conductivity  $\sigma = 5.86 \times 10^7$ .

A model has been setup in a Finite Element Solver (COMSOL) using a 2D TM representation of the geometry shown in Figure 1. Assuming infinite periodicity in the vertical direction, only one single cell of thickness  $p$  has been modeled using Floquet periodicity condition at the top and bottom ends. All the dielectric-metal interfaces are setup with impedance boundary conditions while the LC has been modeled as a dielectric with variable refractive index. Two ports are setup to measure the response of the grating.

### 2.1.1. Amplitude Modulation

When the voltage is applied the refractive index  $n_e$  changes from  $n_{\perp}$  to  $n_{\parallel}$  which increases the effective path length of the channel. The effect is a red shift of the resonances as shown in Figure 3(a). The fact that the field is completely confined within the liquid crystal allows for maximum tunability of the resonance frequencies. For a configuration with  $a = 60 \mu\text{m}$ ,  $p = 300 \mu\text{m}$ ,  $w = 1500 \mu\text{m}$  and an applied voltage from 0 to  $\sim 10 \text{ V}$ , the maximum tunability is around 40 GHz at the frequencies of interest as shown in Figure 3(a). The shape of the grating response suggests that the tuning bandwidth could be used for amplitude modulation (AM) applications or band-pass filters.

On one hand, for AM the requirement is a large change in the transmission as a function of applied voltage. On the other hand, a good band-pass filter requires high transmission in the pass-band and high attenuation in the stop band. Multiple gratings can be placed in a cascade configuration to improve filter performance. The second plot in Figure 3 shows how the filter response changes to a flat-top type with high attenuation in the stop band by using as few as 4 gratings in cascade configuration. One of the pass bands centered at  $\sim 0.443 \text{ THz}$  is enlarged in the figure inset.

Based on the kind of application, the device geometry can be adjusted according to its specific needs. The length  $w$  of the channel typically sets the center frequency of the resonances around which the grating can be tuned. The thickness of the LC layer  $a$ , relative to the period  $p$ , determines the finesse of the filter and increases or decreases the losses due to metal conductivity. The natural amplitude modulation characteristic can be smoothed by using a thicker LC layer; note that this would reduce the LC switching speed, as it behaves inversely proportional to the square of the thickness. Figure 4 shows how the response of the grating changes with the change of the ratio  $a/p$ .

The graphical representation in Figure 4(a) shows both the variation of the response with frequency

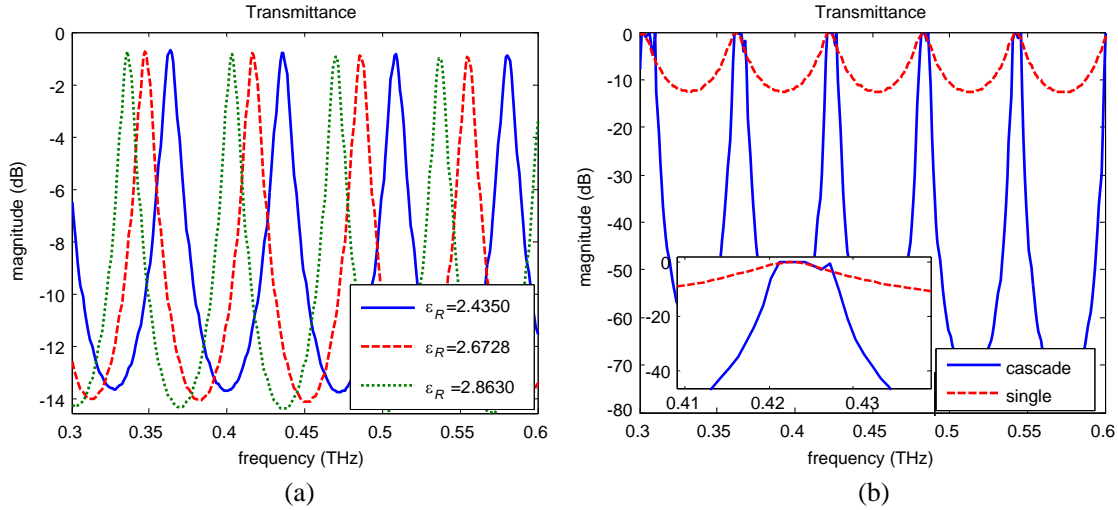


**Figure 3.** (a) Transmittance of metallic grating with the variation of LC permittivity. (b) Transmittance of a cascade of 4 metallic gratings with  $130 \mu\text{m}$  separation ( $a = 60 \mu\text{m}$ ,  $p = 300 \mu\text{m}$ ,  $w = 1500 \mu\text{m}$ ,  $\epsilon_R = 2.6728$ ,  $\sigma = 5.86 \times 10^7$ ).

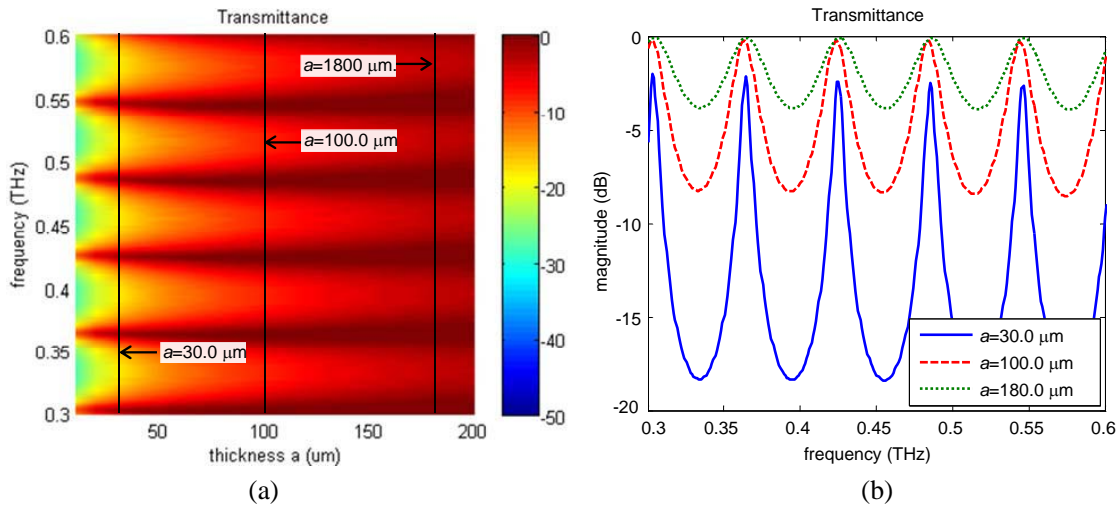


**Figure 4.** Transmittance of metallic grating with varying LC layer thickness ( $p = 300 \mu\text{m}$ ,  $w = 1500 \mu\text{m}$ ,  $\epsilon_R = 2.649$ ,  $\sigma = 5.86 \times 10^7$ ).

and with the thickness  $a$ . Each vertical line in the plot in Figure 4(a) corresponds to a curve shown in the plot Figure 4(b).

A sample of the metallic grating configuration has been manufactured using Copper plates separated by a thin layer of Kapton tape. An area of approximately  $1 \text{ cm}^2$  in the middle was not covered with tape so it can be filled with LC. Both sides of each metallic plate are treated by covering them with a Polyvinyl Alcohol (PVA) solution and then the plates are heated up to  $90^\circ\text{C}$ . After cooling down, both sides of each plate are rubbed in opposite direction. This will force a pre-orientation of the liquid crystal axis director  $\hat{n}$  along the direction of propagation  $\hat{k}$ . The plates are then cut in the middle part in order to obtain the length needed for the experiment ( $\sim 1800 \mu\text{m}$ ). The plates are placed on top of each other and secured in a mount.

Figure 5 shows measurement of the grating using a TM field at normal incidence and the simulated results using COMSOL. The plot shows a very good match for the resonance position in the measurement versus simulated data. The different attenuation in between resonances is probably due to unpredicted resonances excited by the metallic structure holding the grating.

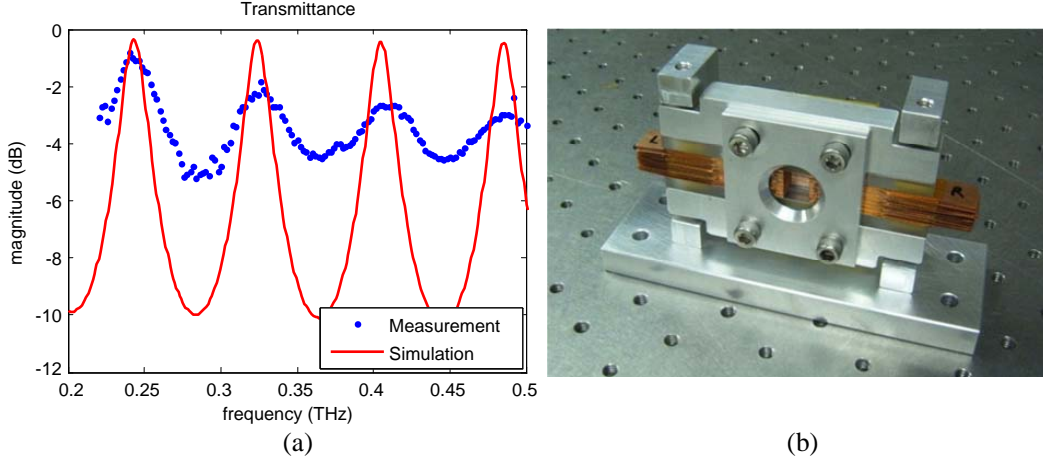


**Figure 5.** (a) Measured transmittance and (b) photo of metallic grating with no LC ( $a = 50.8$ ,  $p = 304.8 \mu\text{m}$ ,  $w = 1800 \mu\text{m}$ ,  $\varepsilon_R = 1$ ,  $\sigma = 5.86 \times 10^7$ ).

### 2.1.2. Phase Modulation Using Brewster Incidence

The previous section showed how a metallic grating filled with LC can be used for amplitude modulating and frequency filtering at the THz regime. In this section the same grating is used as a phase modulator. In general requirements for phase modulation are high transmission over a wide bandwidth and large tunable phase shift.

Using similar configuration as the one studied by de Ceglia et al. [10] at optical frequencies and by Lo Forti et al. at terahertz frequencies [11], a TM field incident on a zero-order metallic grating at a grazing angle demonstrates 100% transmission over an ultra-wide bandwidth. According to Brewster theory, for a single state of polarization an incident angle exists at an interface between two materials with different refractive index for which no reflection is allowed and the signal is totally transmitted. For the grating this incident angle can be calculated using the formula  $\tan(\theta) = n_{eq}/n$  with  $\theta$  incident angle,  $n$  the refractive index of the outside medium and  $n_{eq}$  equivalent refractive index of the grating. A way to approximate the grating equivalent refractive index is by calculating the parallel between the refractive index of the LC and the refractive index of the metal, weighting each term by the surface ratio at the interface.

$$n_{eq} = \left( \frac{a}{p} \frac{1}{n_{LC}} + \frac{p-a}{p} \frac{1}{n_{metal}} \right)^{-1} \quad (2)$$

Using Copper as the metal, an average refractive index value for E7, an LC thickness  $a = 30 \mu\text{m}$  and a grating period  $p = 150 \mu\text{m}$ , the equivalent refractive index is  $n_{eq} \approx 8.113$ . By substituting this value into the Brewster angle formula we have  $\theta_{Brewster} = \text{atan}(8.113) \approx 82.97$  degrees. Numerical results show for this configuration a total transmission at angles around 83 degrees as shown in Figure 6.

Another way to calculate the Brewster angle is solving the associated mode coupling problem. The incidence mode has an impedance equal to  $Z_{in} = \eta_0/np \cos(\theta)$  with  $\eta_0$  characteristic impedance of the vacuum,  $n$  refractive index of the outside medium,  $p$  grating period and  $\theta$  incidence angle. The  $\text{TM}_0$  guided mode inside the grating is confined within the LC layer and has impedance equal to  $Z_{grating} = \eta_0/n_{LC}a$  with  $n_{LC}$  refractive index of the LC and  $a$  LC thickness. The impedance matching condition is achieved when the two impedances are the same. This condition results in:

$$\cos \theta = \frac{a}{p} \frac{n}{n_{LC}} \quad (3)$$

By calculating this formula with the grating parameters previously defined we have  $\theta_{Match} = \text{acos}(30/150 * 1/\sqrt{2.649}) \approx 82.94$  degrees in line with the previous result. As noted in [10] the Brewster angle is quite independent on the change of the LC refractive index.

Incidence at grazing angle forces the response of the grating to be ultra-wide band and phase tunable with the use of LC making it suitable for phase modulation. A grazing incidence angle, though,

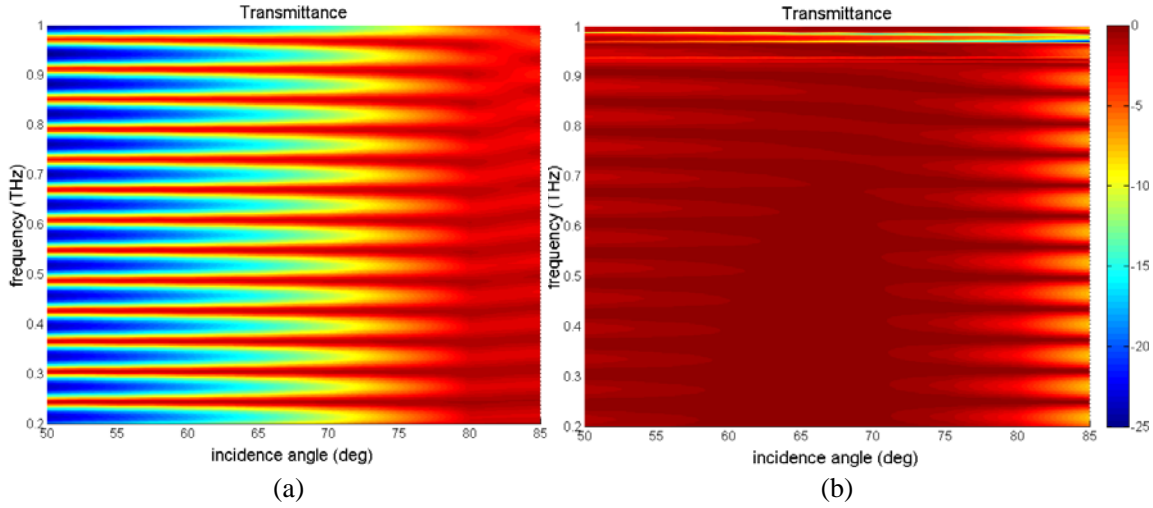


**Figure 6.** Transmittance with the variation of incident angle for (a) a grating with a small LC thickness and (b) a large LC thickness ( $a = 30 \mu\text{m}$  and  $100 \mu\text{m}$ ,  $p = 150 \mu\text{m}$ ,  $w = 1500 \mu\text{m}$ ,  $\epsilon_R = 2.649$ ,  $\sigma = 5.86 \times 10^7$ ).

can considerably complicate the geometry of the grating. The illumination system has to be able to focus the beam on a narrow spot with low spillover due to the top/bottom surface of the grating being close to the edge of the beam. Also, due to the non-zero width of the beam, the area illuminated is elongated across the grating. To avoid losses in the transmittivity the grating height has to be large enough to include the illuminated area which could increase up to 5 or 6 times with respect to normal incidence.

Two different ways to reduce the incidence angle value are investigated, both based on the definition of Brewster angle. The first is to reduce the equivalent refractive index of the grating; the second is to increase the refractive index of the outside medium.

As shown in Formula (3), the Brewster angle depends on the ratio  $a/p$  and the ratio  $n/n_{LC}$ . By increasing the LC thickness with respect to the metal, the angle will decrease. In the example in Figure 6 *a* is increased to  $100 \mu\text{m}$  while keeping the same period  $p$ . The grating in this new configuration is made mostly of liquid crystal. The new Brewster angle can be calculated using Formula (3) as  $\theta_{Match} = \text{acos}(100/150 * 1/\sqrt{2.649}) \approx 65.82$  degrees. A similar number can be calculated by first calculating the equivalent refractive index with Formula (2) resulting in  $n_{eq} \approx 2.44$  and then applying the Brewster angle formula  $\theta_{Brewster} = \text{atan}(2.44) \approx 67.71$  degrees. The new Brewster angle is numerically calculated using COMSOL and it results reduced to  $\sim 66/67$  degrees as shown in Figure 6.

An important factor to notice is that the range of angles for which the device experiences total transmission increased from a few to several degrees. This allows for more tolerance in the setup of the device. Also, being the LC the medium dominating the effective refractive index, a hypothesis could be made that the wideband transmission of the grating is influenced by the change of LC refractive index. By substituting the maximum and minimum permittivity values for E7 in Formula (3) the impedance match angle varies from 64.7 to 66.8 degrees that is well within the flat band area. Numerical simulations confirm this result.

The second solution consists in acting on ratio  $n/n_{LC}$  in Formula (3) increasing the refractive index of the medium outside the grating. Any dielectric with a high refractive index and transparent to THz can be used. Teflon for example has a permittivity equal to about 2.1 at THz frequencies. In order to avoid a change in the propagation vector at the interface between air and the dielectric a prism can be used in between the source and the grating. As done before, the new Brewster angle can be calculated using Formula (3) as  $\theta_{Match} = \text{acos}(30/150 * \sqrt{2.1}/\sqrt{2.649}) \approx 79.7$  degrees. A similar number can be calculated by first calculating the equivalent refractive index with Formula (2) as  $n_{eq} \approx 8.1135$  and then applying the Brewster angle formula  $\theta_{Brewster} = \text{atan}(8.1135/\sqrt{2.1}) \approx 79.9$  degrees. Numerical results show total transmission at angles around 79/80 degrees for this configuration. The phase tunability

reachable with this configuration is  $\sim 130$  degrees with a length  $w = 1500 \mu\text{m}$ .

The two ideas can be combined to further reduce the angle to incidences close to  $\sim 50$  degrees.

## 2.2. Distributed Bragg Feedback

In the previous sections it has been showed how a metallic grating can be used as amplitude modulator or phase modulator with the use of grazing incidence. In the following the basic structure is modified to obtain a wider selection for amplitude modulation or to achieve a flat band response without the use of grazing angles.

A way to modify the natural Fabry-Perot amplitude response of the grating is to stimulate different modes within the slit. The method consists in exciting Bragg modes within each single waveguide by creating small cuts or obstacles in the waveguide itself. The number and the mutual distance of these obstacles affect the overall response of the device.

In order to understand the effect of such features on the overall device response, a simple configuration has been studied. The configuration is shown in Figure 7 and consists in a single cut in the middle of each plate orthogonally to the direction of propagation, similarly to what done by Lockyear et al. [12] at microwave frequencies for a single cell. The length of the cut is  $l$  and the depth is  $d$ .

Numerical simulation results show how this particular configuration induces a shift in the etalon resonance frequencies. This shift is the effect of the mismatch in the middle of the channel caused by the cut. As shown in Figure 8(a), the shift of the resonances varies with the cut length in a sinusoidal shape function of the length of the cut. The period of the sinusoid is a function of the permittivity of the liquid crystal while the main factor that determines the amplitude of the sinusoid is the depth of the cut. The frequencies that do not resonate are largely attenuated; the attenuation increases by increasing the number of cuts. This behavior can be explained with the use of coupled mode theory. In the area with cuts, the forward mode couples with the same mode traveling in the opposite direction ( $-k$ ). For a range of frequencies the imaginary part of the wave number increases in the region and most of its energy is transferred to the backward coupled mode. This results in a frequency range known as “forbidden region” or “band-gap” in solid state physics; within this range the transmission is close to zero and the signal is totally reflected [13].

An increase in the number of cuts/obstacles differently shapes the resonances variation with the length  $l$ . The forbidden region increases in size and pushes the FP resonances towards each other as shown in Figure 8(b) where two cuts on both sides of the plates are placed equispaced from each other and from the edges.

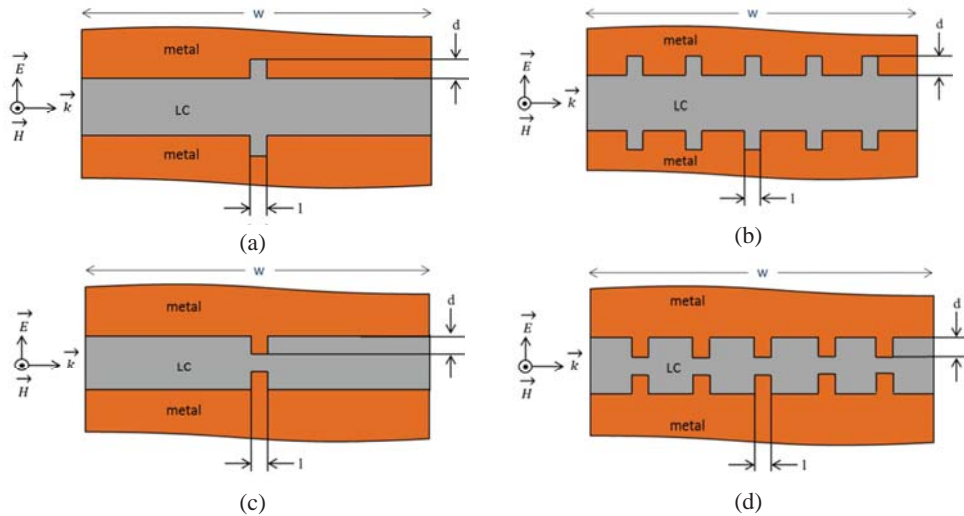


**Figure 7.** Metallic grating with (a) one and (b) multiple cuts and with (c) one and (d) multiple obstacles.

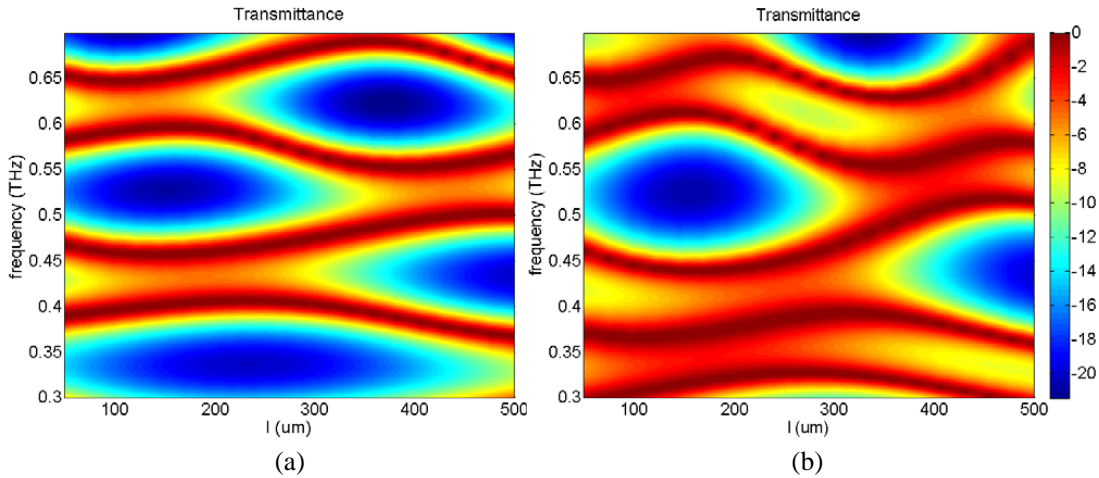


**Figure 8.** Transmittance of metallic grating with (a) one cut in the middle and (b) two cuts equispaced from each other and from the edges as a function of frequency and width of the cuts ( $a = 60 \mu\text{m}$ ,  $p = 300 \mu\text{m}$ ,  $w = 1500 \mu\text{m}$ ,  $d = 30 \mu\text{m}$ ,  $\epsilon_R = 1$ ,  $\sigma = 10^{12}$ ).

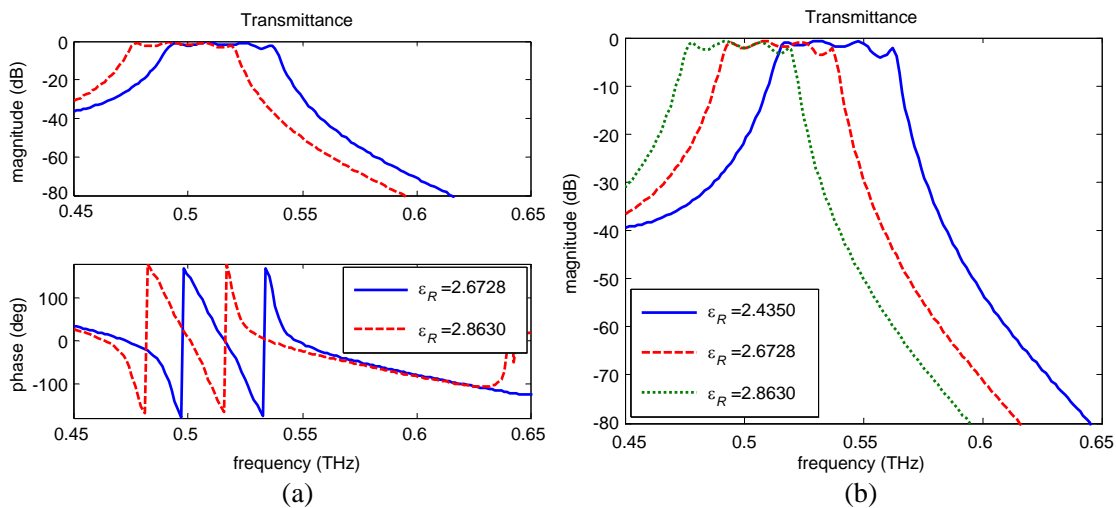


**Figure 9.** Transmittance of metallic grating with 3 equispaced cuts tuned within (a) half the range and (b) the whole range of E7 permittivity values ( $a = 60 \mu\text{m}$ ,  $p = 300 \mu\text{m}$ ,  $w = 1500 \mu\text{m}$ ,  $d = 70 \mu\text{m}$ ,  $l = 50 \mu\text{m}$ ,  $\sigma = 5.86 \times 10^7$ ).

A similar effect in a 2D periodic structure within a PPWG has been already used in [14] to tune the extent of the forbidden region by regulating the air gap between the plates through a series of MEMs actuators.

*2.2.1. Amplitude and Phase Modulation*

One of the important results from the previous section consists in adding a new parameter  $l$  for optimizing the response of the device. In a simple metallic grating the shift of the FP resonances can be achieved by increasing or decreasing the length of the channel  $w$ . The same parameter, though, is the main driving factor for the tunable range of the grating. Introducing this new configurable parameter helps adjusting the response without interfering with the tunability range.

For phase modulation application, in order to achieve a wideband transmission the natural selectivity of the grating response has to be tuned. By increasing the depth of the cuts some of these resonances fuse together. This effect is shown in Figure 9 where four resonances fuse together

to form a wide pass-band. In this configuration the pass-band average attenuation is  $\sim 1.5$  dB with a ripple of  $\sim 1.5$  dB for most of the bandwidth. While the flat-band region is suitable for filtering or phase modulation, the steep slope response is suitable for amplitude modulation or switching applications. Stop-band attenuation can be as low as 60 dB or less thanks to the band-gap effect. The phase response is quite linear in the pass-band. Using the full extent of the LC permittivity variation, the amplitude tunability can reach 30 dB to  $\sim 60$  dB in the slope portion, basing on the linearity requested by the specific application. The phase tunability reaches  $\sim 150$  degrees in the pass-band and it can be extended by increasing the length of the grating  $w$ . The intersection of the flat-bands per different permittivity values determines the usable phase modulation bandwidth. By reducing the range of values for  $\epsilon_R$  the flat-band size increases; reducing, though, the phase tunability.

### 3. DIELECTRIC GRATING

As previously noted the large amount of metal in the device causes an impedance mismatch at the interface that leads most of the energy to be reflected back and for this reason the device becomes frequency selective. In order to use the grating in phase modulation applications a wide pass-band is required. The idea is to reduce the amount of metal in the electrodes in order to reduce the mismatch at the interface and allow for a wider transmit bandwidth. In the previous sections it has been shown how increasing the thickness of the LC layer, with respect to the period, results in widening the pass-band. The downside of that is a slower response of the LC when a voltage is applied. By reducing the period and maintaining the same LC thickness the same result can be achieved driving, though, an increased complexity of the device due to the higher number of plates and LC layers to be overlaid on top of each other. A different approach consists in substituting the electrodes with a transparent dielectric and reducing the metal to two thin layers on both ends of the dielectric to act as electrodes. This new configuration has a lower equivalent refractive index that highly depends on the refractive index of the dielectric used. The radiation, though, is no longer confined in the LC layer being the dielectric permeable to radiation. For this reason, achieving the same extent of tunability with this device requires the propagation distance to be 2 to 4 times longer.

#### 3.1. Continuous Electrodes

The configuration of the unit cell of the grating consists in a layer of transparent dielectric and a layer of LC in between two thin metal layers as shown in Figure 10(a). The metal electrodes, even if thin, results in a periodic transversal structure of parallel plate waveguides. This new structure is made of alternated PPWGs of different thickness and filled alternately with a transparent dielectric and LC.

This new structure shows a higher transmission on average (see Figure 11(a)) with respect to the nominal metallic grating transmission. The transmission, though, shows high reflection lines with close to 100% of the energy reflected. This is the effect of strong coupling at the input and output of the grating between the dielectric and LC channel. The electric field, in fact, is not anymore confined in the liquid crystal but it is also transmitted through the dielectric layers.

The incoming field sees an alternate series of LC and dielectric layers with a thin metal in between. The grating can be modeled as a series of two-port networks. Due to the periodicity of the structure the number of two-port networks can be limited to two; one representing the LC layer and one the dielectric layer. The  $ABCD$  matrix and the scattering matrix for each network can be easily calculated modeling

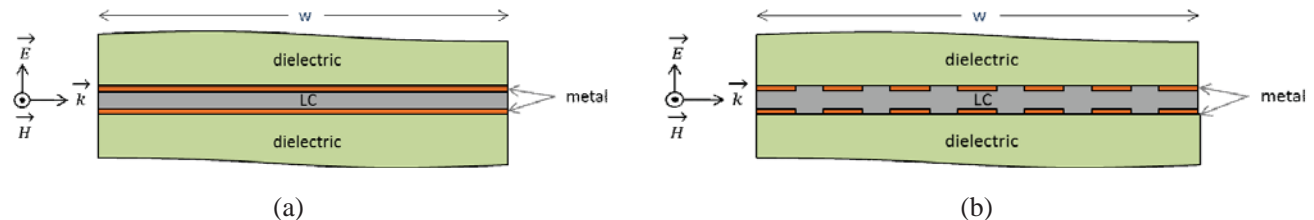


**Figure 10.** Dielectric grating with continuous and non-continuous electrodes.

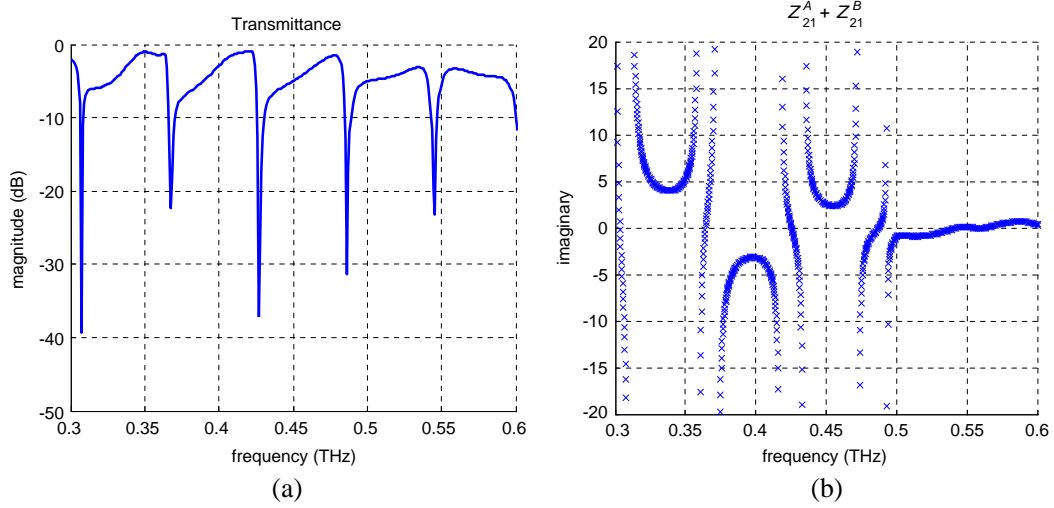


**Figure 11.** Transmittance of the dielectric grating with continuous electrodes and imaginary part of the sum of the two-port network impedances showing the zero-crossing ( $a = 60 \mu\text{m}$ ,  $p = 300 \mu\text{m}$ ,  $w = 1500 \mu\text{m}$ ,  $\varepsilon_R = 2.6490$ ,  $\sigma = 10^{12}$ ,  $\varepsilon_{R,dielectric} = 2.1$ ).

both the LC and dielectric layer as PPWGs. The resulting network is the series of the two two-port networks. The condition of total reflection exists when the scattering parameter  $S_{21}$  of the combined network is equal to zero. Using the scattering to impedance transformation formula  $S_{21} = 2Z_{21}Z_0/\Delta Z$ , this means that the impedance  $Z_{21}$  is zero. The impedance of a series of two-port networks is calculated as the sum of the two impedances  $Z_{21}^{(A)}$  and  $Z_{21}^{(B)}$  of the LC and dielectric layer respectively:

$$Z_{21} = Z_{21}^{(A)} + Z_{21}^{(B)} = 0 \quad \rightarrow \quad Z_{21}^{(A)} = -Z_{21}^{(B)} \quad (4)$$

This means that the two impedances have the same absolute value and a phase difference of 180 degrees. In terms of scattering parameters it can be written:

$$\frac{S_{21}^{(A)}}{(1 - S_{11}^{(A)})^2 - (S_{21}^{(A)})^2} = -\frac{S_{21}^{(B)}}{(1 - S_{11}^{(B)})^2 - (S_{21}^{(B)})^2} \quad (5)$$

By solving Equation (5) or Equation (4) it is possible to approximate the frequency of the notches as shown in Figure 11. The notches in Figure 11(a) are in correspondence to the crossing of the zero line by the function  $Z_{21}^{(A)} + Z_{21}^{(B)}$  in Figure 11(b).

In this particular geometry each dielectric layer is  $\sim 220 \mu\text{m}$  thick while the LC layer is  $60 \mu\text{m}$  thick.

### 3.2. Non Continuous Electrodes

In the previous section it has been exposed how the grating response is widened by substituting the electrodes with a transparent dielectric. The response shows low transmission at certain resonances due to coupling between the two layers at the input and output of the grating and can be approximated by using two two-port devices in a series configuration. In order to avoid a strong coupling at the output at determined frequencies, the idea is to break the uniformity of the structure and let the two waveguide couple along the grating length in order to reduce the change to have a small number of frequencies highly attenuated. To achieve this, the continuous metal electrodes are replaced with non-continuous electrodes obtained by cutting the metal layer perpendicularly to the direction of propagation. The structure is transformed from a series of isolated waveguides coupling at the extremes to a series of waveguides coupled with each other within the grating along the direction of propagation as shown in Figure 10(b).

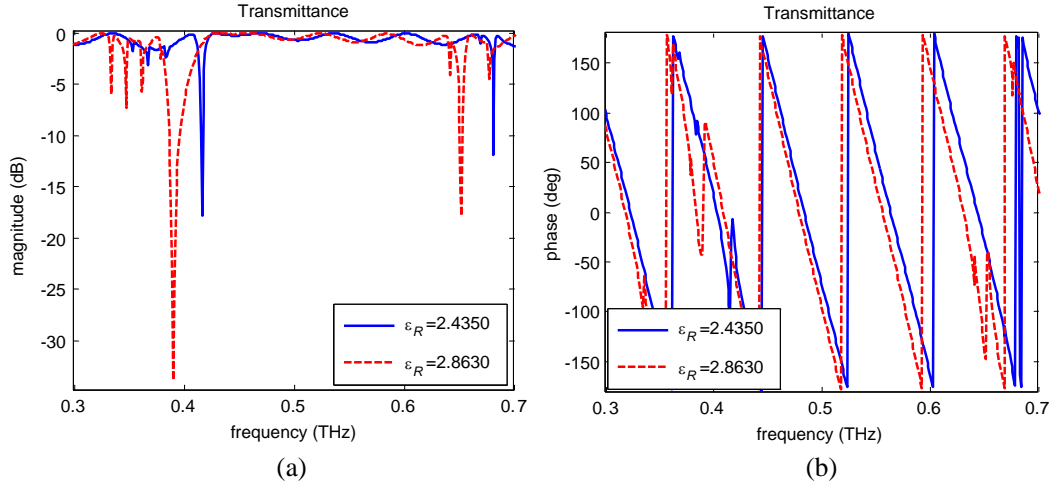


**Figure 12.** (a) Magnitude and (b) phase of the transmission coefficient of the dielectric grating with non-continuous electrodes ( $a = 60 \mu\text{m}$ ,  $p = 300 \mu\text{m}$ ,  $w = 1500 \mu\text{m}$ ,  $\sigma = 5.86 \times 10^7$ ,  $\epsilon_{R\_dielectric} = 2.1000$ ).

### 3.2.1. Phase Modulator

Numerical results for this new configuration show that the coupling has the effect of reducing the depth of the FP resonances increasing the overall transmission. As shown in Figure 12 the transmission of this device is over 80% for a wide range of frequencies and the reflection lines are not present. The magnitude response is very similar to the response of the dielectric layer with a shift that depends on the LC layer refractive index. By changing the LC refractive index, in fact, the whole magnitude response slightly shifts. The phase response in the pass-band is linear and shifts as the LC refractive index changes. The example in Figure 12 shows how a change in the LC permittivity from 2.4350 to 2.8630 causes a phase shift that varies with frequency between 30 and 90 degrees for a grating  $1500 \mu\text{m}$  long.

The tunability of the device can be widened by increasing the length of the grating considering the extra loss due to the metal absorption. Another method is to reduce the dielectric layer thickness or increase its refractive index. This would allow more energy to be guided through the LC layer and to be tuned by the change in the refractive index.

## 4. CONCLUSION

Two different configurations of a transverse stratified structure have been designed to achieve electrically tunable filtering, amplitude and phase modulation at THz frequencies. A metallic grating of plates with layers of LC in between has been studied first. The structure shows FP like response suitable for pass-band filtering when placed in a cascade configuration. The use of incidence at grazing angles in combination with a reduced metal thickness and incidence with a high index dielectric prism forces an impedance matching between the grating and the medium outside widening the transmit bandwidth. The resulting response allows the grating to be used as phase modulator.

A modified version of the grating including cuts or obstacles in the metal plate has been studied. These features excite a backward mode (Bragg regime) within the LC layer causing the FP frequencies to shift without changing the length of the grating. By tuning the size and spacing of the cuts, multiple resonances can be fused together in a wider pass-band suitable for phase modulation. The steep slope in the response resulting from the band-gap effect of the Bragg mode can be used for amplitude modulation applications.

A different configuration using a transparent dielectric in between two thin metal layers in place of the plates has been studied. The dielectric layer allows most of the energy to be transmitted but shows very low transmission in correspondence to FP resonances due to coupling at the extremes. By producing multiple cuts in the metal layer the LC and dielectric layers couple with each other within

the grating and the FP resonances weaken allowing for high transmission over a wide bandwidth that is suitable for phase modulation.

The metallic grating shows a larger tunability than the dielectric grating thanks to the energy being all confined within the LC medium.

## ACKNOWLEDGMENT

The authors would like to acknowledge Ted Rogers, Chris Underwood and Dan Ke in the Center for Applied Optics for assistance in manufacturing the grating and Michael Scalora for the technical expertise. This work was supported by Charles M. Bowden Research Laboratory, AMRDEC, US Army RDECOM.

## REFERENCES

1. Pan, R.-P., C.-Y. Chen, C.-F. Hsieh, and C.-L. Pan, "A liquid-crystal-based terahertz tunable lyot filter," *Appl. Phys. Lett.*, Vol. 88, 101107-1–101107-3, 2006.
2. Mendis, R., A. Nag, F. Chen, and D. M. Mittleman, "A tunable universal terahertz filter using artificial dielectrics based on parallel-plate waveguides," *Appl. Phys. Lett.*, Vol. 97, 131106, 2010.
3. Unlu, M., C. W. Berry, S. Li, S.-H. Yang, M. R. Hashemi, and M. Jarrahi, "Broadband terahertz modulation using reconfigurable mesh filters," *2013 IEEE 14th Annual Wireless and Microwave Technology Conference (WAMICON)*, 1–3, Apr. 7–9, 2013.
4. Zhu, W. M., H. Cai, T. Mei, T. Bourouina, J. F. Tao, G.-Q. Lo, D.-L. Kwong, and A. Q. Liu, "A MEMS tunable metamaterial filter," *2010 IEEE 23rd International Conference on Micro Electro Mechanical Systems (MEMS)*, 196–199, Jan. 24–28, 2010.
5. Wu, H.-Y., C.-F. Hsieh, T.-T. Tang, R.-P. Pan, and C.-L. Pan, "Electrically tunable room-temperature  $2\pi$  liquid crystal terahertz phase shifter," *IEEE Photonics Technology Letters*, Vol. 18, No. 14, 1488–1490, Jul. 2006.
6. Yang, F. and J. R. Sambles, "Microwave liquid crystal wavelength selector," *Appl. Phys. Lett.*, Vol. 79, No. 22, 3717–3719, Nov. 2001.
7. Medina, F., F. Mesa, and D. C. Skigin, "Extraordinary transmission through arrays of slits: A circuit theory model," *IEEE Transactions on Microwave Theory and Techniques*, Vol. 58, No. 1, 105–115, Jan. 2010.
8. Yeh, P. and C. Gu, *Optics of Liquid Crystal Displays*, 15–47, Wiley Publishers, Hoboken, New Jersey, 2010.
9. Yang, C. S., C. J. Lin, R. P. Pan, C. T. Que, K. Yamamoto, M. Tani, and C. L. Pan, "The complex refractive indices of the liquid crystal mixture E7 in the terahertz frequency range," *Journal of the Optical Society of America B*, Vol. 27, No. 9, 1866–1873, 2010.
10. De Ceglia, D., M. A. Vincenti, and M. Scalora, "Wideband plasmonic beam steering in metal gratings," *Optics Letters*, Vol. 37, No. 2, 271–273, 2012.
11. Lo Forti, D., D. de Ceglia, M. A. Vincenti, M. Scalora, and R. G. Lindquist, "Beaming and filtering at terahertz frequencies in liquid crystal filled metallic grating," *Proc. SPIE 8828, Liquid Crystals XVII*, 88281E, Sep. 12, 2013.
12. Lockyear, M. J., A. P. Hibbins, and J. R. Sambles, "Transmission of microwaves through a stepped subwavelength slit," *Appl. Phys. Lett.*, Vol. 91, No. 25, 251106-1–251106-3, Dec. 2007.
13. Zhao, Y. and D. Grischkowsky, "A new method for the realization of a tunable terahertz photonic bandgap," *Conference on Lasers and Electro-Optics, CLEO 2007*, 1–2, May 6–11, 2007.
14. Loewen, E. G. and E. Popov, *Diffraction Gratings and Applications*, M. Dekker Publisher, New York, 1997.